*Journal of Sound and Vibration* (1998) **210**(1), 37–52

# AN ANALYTICAL STUDY OF FUZZY CONTROL OF A FLEXIBLE ROD MECHANISM

D. BEALE

*Department of Mechanical Engineering, Auburn University, Alabama* 36849, *U.S.A.*

S. W. LEE

*Chin Min College, Taiwan, Republic of China*

AND

D. BOGHIU

*Mathworks Inc., Natick, MA* 01760, *U.S.A.*

(*Received* 25 *April* 1997, *and in final form* 18 *August* 1997)

The non-linear nature of very high speed, flexible rod mechanisms has been previously confirmed, both experimentally and analytically in reference [1]. Therefore, effective control system design for flexible mechanisms operating at very high speeds must consider the non-linearities when designing a controller for very high speeds. Active control via fuzzy logic is assessed as a means to suppress the elastic transverse bending vibration of a flexible rod of a slider crank mechanism. Several pairs of piezoelectric elements are used to provide the control action. Sensor output of deflection is fed to the fuzzy controller, which determines the voltage input to the actuators. A three mode approximation is used in the simulation study. Computer simulation shows that fuzzy control can be used to suppress bending vibrations at high speeds, and even at speeds where the uncontrolled response would be unstable.



## 1. INTRODUCTION

The design and vibration control of flexible linkage mechanisms has been much investigated in the recent literature. One method of designing links is by cross-sectional geometry optimization [2, 3]. Another method was proposed by Sung and Thompson [4], who proposed the use of modern composite materials for flexible linkage design because of their superior damping and high stiffness to weight ratios. These two aforementioned design approaches can be classified as passive vibration control. Oliver *et al*. [5] introduced an active vibration control scheme incorporating a microprocessor controlled actuator included in the original mechanism to reduce the midspan deflection of the flexible linkages.

Advances in composite technology—including materials such as optic fibers, piezoelectric ceramics and polymers—can be bonded or embedded in composite laminates and structures and may play a significant role in active vibration control. Flexible linkage mechanisms equipped with these materials (as sensors and actuators) and possessing computational and control capacities may be classified as smart mechanisms [6].

Bailey and Hubbard [7] designed an active vibration damper using piezoelectric actuators and distributed parameter control theory. Theoretical and experimental studies

0022–460X/98/060037 + 16 $25.00/0/sv971266 

on multi-layered thin shells coupled with piezoelectric shell actuators for distributed vibration control were performed by Tzou and Gadre [8].

Sung and Chen [9] employed a state feedback optimal control scheme to suppress the elastodynamic responses of a high speed four bar mechanism. A Luenberger observer was also included for states estimation. The instabilities caused by the combined effect of the control and observation spillover were investigated and prevented. Lee *et al*. [10] developed a variational theorem for the finite element analysis and control of flexible linkage systems using piezoelectric ceramic actuators.

Liao and Sung [11] presented an analytical and experimental study on the elastodynamic analysis and control of a four bar mechanism using piezoceramic sensors and actuators. A linear quadratic Gaussian regulator with a loop transfer recovery control scheme was designed to control the motion of a four bar linkage mechanism with one flexible link. The results obtained showed that the midspan vibration of the flexible link was greatly suppressed and the spillover instability can be avoided. However, non-linearities were not considered in controller design in either reference [9] or [11], because the speeds were low.

Thompson and Tao [12] experimented with a flexible slider crank mechanism using piezoceramic actuators and strain gage sensors. In one effective scheme, sensor output was amplified and fed back to the piezoceramics, with gains perhaps determined by a trial-and-error procedure. Because there is no analytical controller design in reference [12], one conjectures that controller gains were chosen via an informal trial-and-error procedure based on error rather than model-based as in references [9] and [11]. These sorts of procedures are formally employed in fuzzy logic controller design (i.e., trial-and-error membership function determination and an error-based design instead of model-based), which is firmly rooted in fuzzy mathematics. Their work bolsters our contention that fuzzy logic control is worth investigating for flexible mechanisms.

Fuzzy logic control is a non-linear control that has been applied in a wide variety of control applications. Applications include consumer products, such as washing machines that can set the cycle time for the amount of dirt in clothes and load size. Research applications most resembling flexible mechanisms like slider cranks include flexible links on robots requiring control for accurate positioning [13, 14]. Generally speaking, fuzzy logic control is justified for both linear and non-linear systems because precise mathematical models inadequately describe the real world device the model had been intended to emulate. Founders of fuzzy logic control recognized that classical control placed too much emphasis on precision and precise models, and therefore could not handle complex systems. Conventional model based control has been successfully applied when the dynamics of the plant are well understood, where performance of the plant strongly depends on the operating parameters. However, uncertainties in the model can yield unsatisfactory performance of the conventional controller. Conversely, fuzzy logic controllers are error based controllers that do not depend upon the mathematical model, that is, they are not model based.

In the case of the slider crank and flexible mechanisms, there are mathematical modelling uncertainties. Modelling uncertainties can arise from incomplete mathematical models because of the necessity to create tractable equations; for example slider cranks do not run at an exact constant crank speed, nor are the rods of constant cross-sectional area, the joints are not frictionless, a truncated mode approximation is made, non-linearities are dropped from the analysis, etc. The analytical and experimental response shown in reference [1] demonstrated non-linear behavior such as bifurcations, jumps, and period doubling toward chaos in a flexible mechanism. Equilibrium solutions (needed for linearization for linear controller design methods) are not stationary points but periodic orbits, and dependent upon the operating speed. In theory, a controller must be designed

by linearizing about a particular equilibrium solution; however there can be many in the presence of bifurcations and changing operating crank speeds [15]. In general, controllers designed using linear control theory after linearization for highly non-linear systems have been shown to be limited or ineffective, and possibly unstable. Fuzzy logic controllers can effectively control systems under conditions such as these where other controllers may fail. For these aforementioned reasons, flexible mechanisms are candidates for fuzzy logic control.

Lim and Hiymane [16] proposed proportional–integral and fuzzy logic controllers to control a two link rigid robot. The PI controller was used to ensure fast transient response and zero steady-state error. The fuzzy logic controller was used to enhance the damping characteristics of the system. However, they found that the gains adjustment of the PI controller requires a large effort and the control scheme does not compensate for the non-linear effects of the robot system.

Liu and Lewis [13] designed a feedback–linearization/fuzzy logic hybrid scheme for a robotic manipulator with link flexibility. The control scheme was composed of a feedback–linearization inner-loop control and a fuzzy linguistic outer-loop control. A reduced-order computed torque control was first used to linearize the whole system to a Newton's law-like system, then a linguistic fuzzy controller (of 33 if–then fuzzy rules) was used to command the rigid modes to track a desired trajectory while the residual vibrations were maintained as small as possible.

Kubica and Wang [14] applied a fuzzy control strategy to control the rigid body and the first flexural mode of vibration in a single link robotic arm. Two fuzzy logic controllers were constructed. The first one was designed to govern the rigid motion of the beam as it was rotated from one position to another. The second controller was designed to attenuate the vibrations resulting from the rigid body motion. The results obtained showed an improvement over those obtained using conventional multivariable techniques.

Boghiu and Marghitu [17] employed a fuzzy logic controller to remove the vibrations of a periodic impacting flexible link. The flap motion of the flexible link was analyzed. A fuzzy logic controller was also designed to control the vibrations of a parametrically excited rotating flexible beam [18].

Due to the attractive features of fuzzy logic controllers, this control strategy is also used in this work for vibration suppression of an elastic crank–slider mechanism. Robustness of the fuzzy controller is examined using an external random sine function disturbance. Studies are based on a three mode approximation of rod bending, higher modes being truncated from the analysis; this brings up the issue of spillover which is not discussed in this simulation study. Linear systems methods have been previously proposed to avoid spillover, but this is still an open question for non-linear systems. Challenges in fuzzy logic control include systematic ways to determine membership functions and a development of a stability theory.

## 2. MATHEMATICAL MODEL

### 2.1. SYSTEM MODEL

The diagram of the system is shown in Figure 1. The system consists of a rigid massless link $OA$ (of length $a$) that can rotate in the horizontal plane with a constant angular velocity $\omega$. A flexible link $AB$ connects the link $OA$ with a piston. The flexible beam has length $L$, a constant flexural rigidity $EI$ and a uniformly distributed mass per unit length $\rho = m/L$, where $m$ is the total mass of the beam. The piston, of mass $M_s$, can slide in the horizontal direction and $P_s$ is an applied force (e.g., gas force).

Two reference frames are considered: a "fixed" reference frame ($N$), of unit vectors **i**, **j** and **k**, whose origin is at $O$, and a "mobile" reference frame ($R$), of unit vectors $\mathbf{e}_1$, $\mathbf{e}_2$ and $\mathbf{e}_3$, with the origin at $A$. This frame is attached to the flexible link $AB$, such that the unit vector $\mathbf{e}_1$ is along the undeformed elastic link $AB$, as shown in Figure 1. Let $-\phi$ be the angle between a horizontal line parallel with the **i** vector passing through joint $A$ and the direction of the $\mathbf{e}_1$ vector. The unit vectors are related by the transformation

$$\begin{bmatrix} \mathbf{e}_1 \\ \mathbf{e}_2 \\ \mathbf{e}_3 \end{bmatrix} = \begin{bmatrix} \cos\phi & \sin\phi & 0 \\ -\sin\phi & \cos\phi & 0 \\ 0 & 0 & 1 \end{bmatrix} \begin{bmatrix} \mathbf{i} \\ \mathbf{j} \\ \mathbf{k} \end{bmatrix}. \tag{1}$$

Let $P$ be a current point of the flexible link $AB$. Because the foreshortening effect is considered, let $u$ and $v$ be longitudinal and transversal deflections of the point $P$ from its undeformed position (point $P_0$ on Figure 1). In vector form, these deflections can be written as

$$\mathbf{u} = -P_0 P_1 \mathbf{e}_1 = -u\mathbf{e}_1, \qquad \mathbf{v} = P_1 P \mathbf{e}_2 = v\mathbf{e}_2. \tag{2}$$

Let $x$ be the distance from the point $A$ to $P_0$ and $\mathbf{r}_P$ the position vector of point $P$ with respect to origin $O$,

$$\mathbf{r}_P = a\cos\omega t\mathbf{i} + a\sin\omega t\mathbf{j} + (x-u)\mathbf{e}_1 + v\mathbf{e}_2. \tag{3}$$

The transversal deflection $v$ ($P_1 P$ in Figure 1) is computed using the expression

$$v(x,t) = \sum_{j=1}^{n} \Phi_j(x) q_j(t), \tag{4}$$

where $q_j(t)$ are the generalized elastic co-ordinates, and $n$ is the total number of vibrational modes. The functions $\Phi_j(x)$ are chosen as the mode shapes of a pinned–pinned beam and are defined by the expression

$$\Phi_j(x) = \sin(j\pi x/L). \tag{5}$$

The longitudinal deflection $u$ ($P_0 P_1$ in Figure 1), due to the foreshortening effect is given by

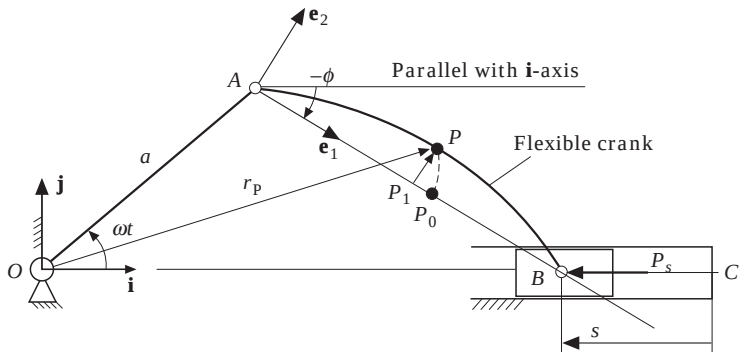


Figure 1. The system model.

$$u = \tfrac{1}{2}\int_0^x \left(\frac{\partial v}{\partial x}\right)^2 \mathrm{d}x. \tag{6}$$

The total kinetic energy $T$ of the system is

$$T = \frac{\rho}{2}\int_0^L \dot{\mathbf{r}}_P \cdot \dot{\mathbf{r}}_P \,\mathrm{d}x + \tfrac{1}{2} M_s \dot{s}^2. \tag{7}$$

Using equation (3), one can get

$$\dot{\mathbf{r}}_P = \mathrm{d}\mathbf{r}_P/\mathrm{d}t = [a\omega \sin(\phi - \omega t) - v\dot{\phi} - u_t]\mathbf{e}_1 + [a\omega \cos(\phi - \omega t) + (x-u)\dot{\phi} + v_t]\mathbf{e}_2, \tag{8}$$

where $u_t$ and $v_t$ are the partial derivatives with respect to time of $u$ and $v$ respectively. Taking into account that the longitudinal deflection $u$ is much smaller than any other distances involved in equation (8), the expression of $\dot{\mathbf{r}}_P$ can be simplified to

$$\dot{\mathbf{r}}_P = \mathrm{d}\mathbf{r}_P/\mathrm{d}t = [a\omega \sin(\phi - \omega t) - v\dot{\phi}]\mathbf{e}_1 + [a\omega \cos(\phi - \omega t) + x\dot{\phi} + v_t]\mathbf{e}_2. \tag{9}$$

The potential energy $U$ of the system is

$$U = \tfrac{1}{2}\int_0^L EI\left(\frac{\partial^2 v}{\partial x^2}\right)^2 \mathrm{d}x - P_s s. \tag{10}$$

The angle $\phi$ and the linear displacement $s$ of the piston can be determined from the geometry of Figure 1, using the vectorial equation

$$\mathbf{OA} + \mathbf{AB} + \mathbf{BC} = \mathbf{OC}. \tag{11}$$

Thus, two constraint equations are obtained:

(1) the **i** component is

$$\Phi_1 = a\cos\omega t + s - a - L + (L - u(L))\cos\phi = 0, \tag{12}$$

where $u(L)$ is the foreshortening value of the point $B$, computed with the expression

$$u(L) = \tfrac{1}{2}\int_0^L \left(\frac{\partial v}{\partial x}\right)^2 \mathrm{d}x. \tag{13}$$

(2) the **j** component is

$$\Phi_2 = a\sin\omega t + (L - u(L))\sin\phi = 0. \tag{14}$$

Because the mechanism has two constraints $\Phi_1$ and $\Phi_2$, Lagrange's equations of motion have the form

$$\frac{\mathrm{d}}{\mathrm{d}t}\frac{\partial T}{\partial \dot{q}_{0,i}} - \frac{\partial T}{\partial q_{0,i}} + \frac{\partial U}{\partial q_{0,i}} = Q_i + \Phi_1\lambda_1 + \Phi_2\lambda_2 + D_i. \tag{15}$$

In equation (15), $\lambda_1$ and $\lambda_2$ are Lagrange multipliers (one for each constraint), $Q_i$ is the vector of generalized non-conservative forces and $D_i$ is the vector of generalized disturbance unmodelled forces. The vector $\mathbf{q}_0$ is defined by

$$\mathbf{q}_0 = [q_1, q_2, \ldots, q_n, \phi, s]^{\mathrm{T}}, \tag{16}$$

and $q_{0,i}$ is the $i$th component of the vector $\mathbf{q}_0$. In this work a three mode approximation ($n = 3$) of the elastic link is considered. The vector $\mathbf{q}_0$ has five components,

TABLE 1

*Properties of piezoelectric material*

| Specifications | Prescribed value | Unit |
|---|---|---|
| Width ($b_p$) | $1{\cdot}905 \times 10^{-2}$ | m |
| Thickness ($t_p$) | $1{\cdot}905 \times 10^{-2}$ | m |
| Young's modulus ($E_p$) | $63 \times 10^{9}$ | $N/m^2$ |
| Strain constant ($d_{31}$) | $180 \times 10^{-12}$ | m/V |

$$\mathbf{q}_0 = [q_1, q_2, q_3, \phi, s]^{\mathrm{T}}. \tag{17}$$

The following equations of motions are obtained:

(1) for the generalized elastic co-ordinates $q_i$, $i = 1, 2, 3$:

$$\tfrac{1}{2}\rho L\ddot{q}_i + (-1)^{i+1}\frac{\rho L^2}{i\pi}\ddot{\phi} + \frac{i^2\pi^2 q_i \cos\phi}{2L}\lambda_1 + \frac{i^2\pi^2 q_i \sin\phi}{2L}\lambda_2 - \frac{\rho L}{2}\dot{\phi}^2 q_i$$

$$+ \frac{i^4\pi^4 EI}{2L^3}q_i + \begin{Bmatrix} 0, & i \text{ even} \\ 2\rho a\omega^2 \sin(\phi - \omega t)L/i\pi, & i \text{ odd} \end{Bmatrix} = F_i + d_{q,i}, \tag{18}$$

where $F_i$ is the force given by the actuators (piezoelectric elements) and its expression will be derived later. The force $d_{q,i}$ is the disturbance force associated with the elastic co-ordinates.

(2) for the angle $\phi$,

$$\sum_{i=1}^{n}(-1)^{i+1}\frac{\rho L^2}{i\pi}\ddot{q}_i + \sum_{i=1}^{n} q_i\dot{\phi}\rho L\dot{q}_i + \left(\frac{\rho L^3}{3} + \sum_{i=1}^{3}\frac{\rho L}{2}q_i^2\right)\ddot{\phi}$$

$$+ \left(L\sin\phi - \sum_{i=1}^{n}\frac{i^2\pi^2 q_i \sin\phi}{4L}\right)\lambda_1 + \left(-L\cos\phi + \sum_{i=1}^{n}\frac{i^2\pi^2 q_i\cos\phi}{4L}\right)\lambda_2$$

$$+ \frac{2\rho a\omega^2 L^2 \sin(\phi - \omega t)}{\pi} + \begin{Bmatrix} 0, & i \text{ even} \\ \sum_{i=1}^{n}\dfrac{2\rho a\omega^2 L q_i \cos(\phi - \omega t)}{i\pi}, & i \text{ odd} \end{Bmatrix} = d_\phi, \tag{19}$$

where $d_\phi$ is the disturbance force associated with the angle $\phi$.

(3) for the co-ordinate $s$,

$$M_s\ddot{s} - P_s - \lambda_1 = d_s, \tag{20}$$

where $d_s$ is the disturbance force associated with the displacement $s$. The second order differential equations (18), (19) and (20) and the algebraic equations (12) and (14) form

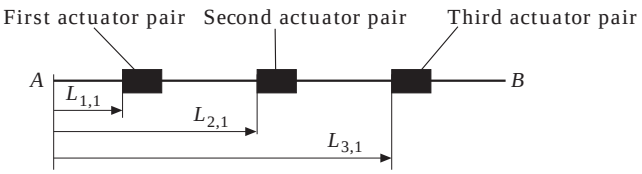


Figure 2. Actuator locations.

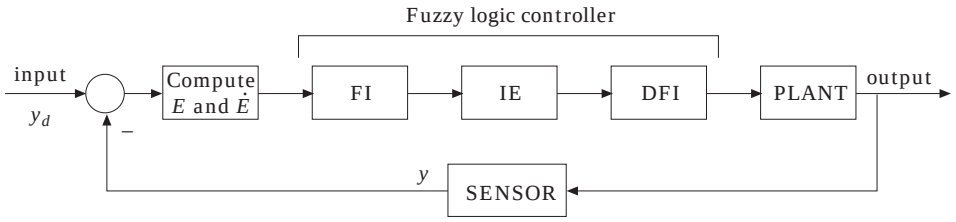


Figure 3. Basic configuration of a fuzzy logic controller.

a system of twelve equations with twelve unknowns: $q_1$, $q_2$, $q_3$, $\phi$, $s$, their time derivatives, as well as $\lambda_1$ and $\lambda_2$.

### 2.2. PIEZO ACTUATOR MODEL

The piezoelectric material is an electromechanical transducer. When an electric field is applied to piezoelectric material, a strain is produced in the material (assuming free boundary conditions). Similarly, if the material is stressed, an electric field is generated. When an electric voltage $U(t)$ is applied, the bending moment produced is [19]

$$M(x, t) = cU(t)\,[\mathrm{h}(x - L_1) - \mathrm{h}(x - L_2)], \tag{21}$$

where $\mathrm{h}(\cdot)$ is the Heaviside step function, and $L_1$ and $L_2$ are the locations of the actuator ends, measured from the joint $A$. The coefficient $c$ is the moment-voltage constant, defined by

$$c = b_p\, d_{31}\, E_p\, (t_b + t_p)/2, \tag{22}$$

and is a function of the piezoelectric material properties, such as $b_p$ (width of the piezoelectric), $E_p$ (piezoelectric Young's modulus), $t_p$ (thickness of a single layer of piezoceramic), $d_{31}$ (piezoelectric strain constant), and $t_b$ (thickness of the beam).

The piezoelectric actuator provides a non-conservative force to the system whose work can be written as [20]

$$W_{nc} = \int_0^L M(x, t)\,\frac{\partial^2 v}{\partial x^2}\,\mathrm{d}x. \tag{23}$$

Three pairs of G-1195 piezoelectric actuators (properties shown in Table 1) manufactured by Vernitron Inc. are attached to the beam shown in Figure 2. The locations of the ends of each actuator pair (measured from point $A$) are: $L_{1,1} = 0{\cdot}2L$, and $L_{1,2} = 0{\cdot}35L$ for the first element, $L_{2,1} = 0{\cdot}45L$ and $L_{2,2} = 0{\cdot}55L$ for the second element and $L_{3,1} = 0{\cdot}65L$ and $L_{3,2} = 0{\cdot}8L$ for the third one. The moment-voltage coefficient $c$ is calculated using equation (22) and has a value of $c = 1{\cdot}6464 \times 10^{-3}$ lbin/volt. $U_1(t)$, $U_2(t)$ and $U_3(t)$ are the voltages applied to each top actuator of the pair, and oppositely to the bottom. The transversal deflection is measured by three sensors, placed at the $x_1 = L/3$, $x_2 = L/2$ and $x_3 = 2L/3$ from the point $A$. These may be strain gages placed on top of the top actuators as in reference [12]. The output of the $k$th sensor ($k = 1, 2, 3$) is the actual transversal deflection of the sensor,

$$y_k = \sum_{j=1}^{3} \Phi_j(x_k) q_j(t). \tag{24}$$

The output from the $k$th sensor is used to generate the input voltage for the $k$th actuator pair.

The total non-conservative work produced by all three actuator pairs is

$$W_{nc,tot} = W_{nc,1} + W_{nc,2} + W_{nc,3} = \int_0^L \left( \sum_{j=1}^{3} M_j(x, t) \right) \frac{\partial^2 v}{\partial x^2} \, \mathrm{d}x. \tag{25}$$

Using equation (25), the generalized non-conservative control force in equation (18) is

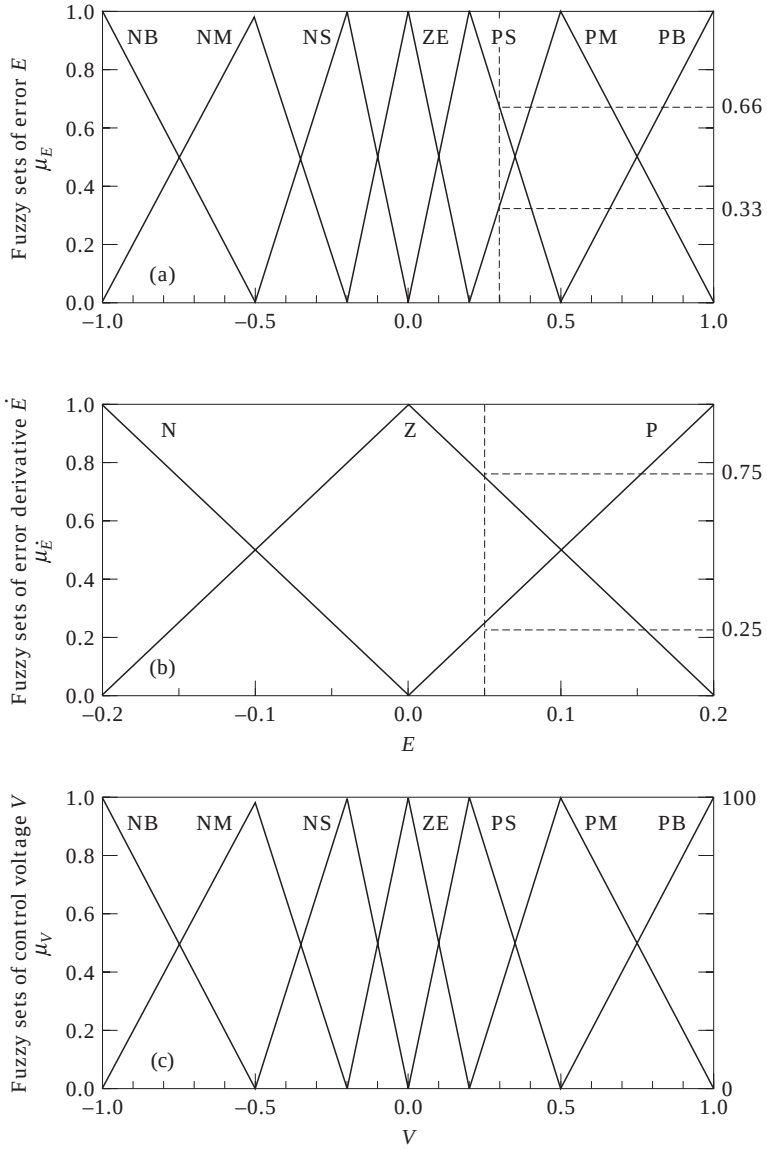


Figure 4. The fuzzy sets of the controller input $E$ in (a), $\dot{E}$ in (b) and output $V$ in (c).

TABLE 2

*Fuzzy control rules*

| $E$ | PB | PM | PS | ZE | NS | NM | NB |
|---|---|---|---|---|---|---|---|
| $\dot{E}$ = P | NM | NM | NS | NS | ZE | PS | PS |
| $\dot{E}$ = Z | NB | NM | NS | ZE | PS | PM | PB |
| $\dot{E}$ = N | NS | NS | ZE | PS | PS | PM | PM |

$$Q_i = c\frac{i\pi}{L}\left[\left(\cos\frac{L_{1,1}\,i\pi}{L} - \cos\frac{L_{1,2}\,i\pi}{L}\right)U_1(t) + \left(\cos\frac{L_{2,1}\,i\pi}{L} - \cos\frac{L_{2,2}\,i\pi}{L}\right)U_2(t)\right.$$

$$\left. + \left(\cos\frac{L_{3,1}\,i\pi}{L} - \cos\frac{L_{3,2}\,i\pi}{L}\right)U_3(t)\right]. \tag{26}$$

## 3. FUZZY LOGIC CONTROL

The diagram of a fuzzy logic controller is shown in Figure 3 [21]. Three identical fuzzy logic controllers (one for each actuator pair) are designed. Each fuzzy logic controller has as inputs the normalized error $E$, defined as the difference between the output of the corresponding sensor ($y$) and the desired value ($y_d$, zero in this case),

$$E = (y - y_d)/GE = y/GE, \tag{27}$$

and the normalized value of the error derivative

$$\dot{E} = \dot{y}/GC. \tag{28}$$

The output of each fuzzy logic controller is the normalized value of the voltage $V$ that can be applied to the corresponding actuator. The actual and normalized voltages are related by the expression

$$U = VGU. \tag{29}$$

Here $GE$, $GC$ and $GU$ are predefined scaling factors.

### 3.1. FUZZIFICATION

During *fuzzification* (the FI block in Figure 3), input variables are associated with a set of linguistic fuzzy variables (e.g., fuzzy error $E$ and fuzzy change in error $\dot{E}$). Fuzzy variables have value—describable not by numbers—but by fuzzy sets (for example NB for Negative Big, etc.). Associated with each fuzzy set are triangular membership functions

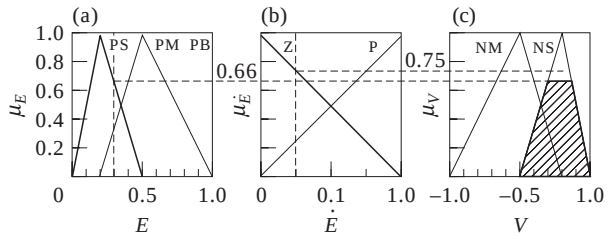


Figure 5. Influence of RULE 1 on output $\mu_E$ in (a), $\mu_{\dot{E}}$ in (b), and $\mu_V$ in (c).

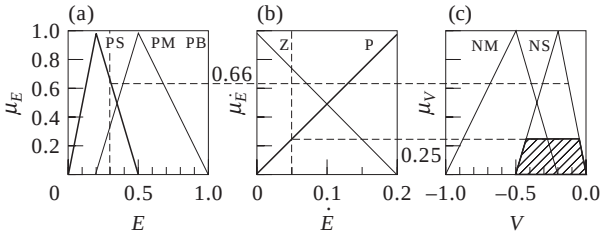


Figure 6. Influence of RULE 2 on output $\mu_E$ in (a), $\mu_{\dot{E}}$ in (b), and $\mu_V$ in (c).

$\mu$, like those shown in Figure 4. The process of associating a numerical value with a fuzzy set is called *fuzzification*. A membership function provides through $\mu$ a measure of the degree of membership a variable has in a given set. The scaling factors $GE$ and $GC$ are chosen such that the minimum and maximum values of $E$ and $\dot{E}$ lie within the aforementioned intervals. These intervals are called the *Universe of Discourse* associated with that particular variable. Individual triangular membership functions will overlap, as one can see in Figure 4. The overlap between the sets allows for a smooth transition between sets. The error $E$ and the normalized output voltage $V$ membership functions have seven sets, defined as positive big (PB), positive medium (PM), positive small (PS), zero (ZE), negative small (NS), negative medium (NM) and negative big (NB). The $\dot{E}$ membership function has 3 sets: positive (P), zero (Z) and negative (N).

As an example, let one consider that for a certain moment of time, the error $E$ and its derivative $\dot{E}$, for one sensor, are 0·3 and 0·05, respectively. From Figure 4, one can see that the error belongs to both positive small (PS) and positive medium (PM) sets, with "grades" $\mu$ of 2/3 and 1/3, respectively (grade being an indication of the degree of partial membership of element $E$ in a linguistic set). A maximum grade of 1 indicates that $E$ belongs entirely to one set. The error derivative $\dot{E}$ belongs to both zero (Z) and positive (P) sets, with grades 0·75 and 0·25, respectively.

It should be mentioned that the fuzzy logic controller design is a heuristic process, and determination of gains $GE$ and $GC$ and the number of fuzzy sets in Figure 4 that make up a membership function is not an analytical procedure, as in classical control system design. The approach taken here was to design a fuzzy controller with a small number of fuzzy sets, but yet with a sufficiently complete rulebase to achieve small rod bending deflections and without exceeding the breakdown voltage of the piezoceramic material (1500 V).

### 3.2. INFERENCE ENGINE

In the inference engine (the IE block in Figure 3), fuzzy control rules (predetermined rules among the fuzzy variables described by IF–THEN statements, and easily presented

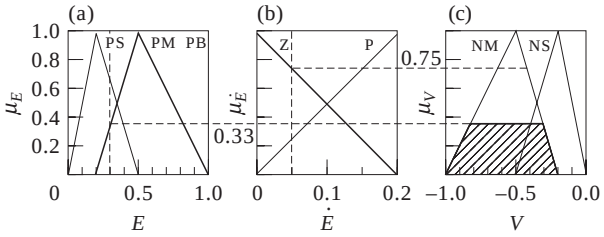


Figure 7. Influence of RULE 3 on output $\mu_E$ in (a), $\mu_{\dot{E}}$ in (b), and $\mu_V$ in (c).

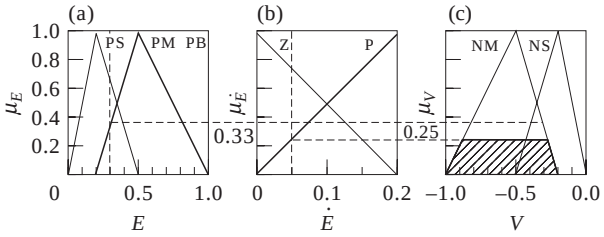


Figure 8. Influence of RULE 4 on output $\mu_E$ in (a), $\mu_{\dot{E}}$ in (b), and $\mu_V$ in (c).

in table form) are applied to determine another fuzzy set to describe the output control action. The inference engine is driven by such a rule-base control scheme, which is usually derived from an operator's experience and/or a control engineer's expertise. In this study, a proportional–derivative type of control action is utilized and has the following IF–THEN conditional statement structure:

$$\text{IF } E_i \text{ is } A_i \text{ and } \dot{E}_i \text{ is } B_i, \text{ THEN } U_F \text{ is } C_i,$$

where $i$ is the $i$th rule, and $A_i$, $B_i$, and $C_i$ are linguistic fuzzy sets in the membership functions for $E_i$, $\dot{E}_i$ and $U_F$ respectively. The control rules used in this study are a combination of $7 \times 3 = 21$ rules as shown in Table 2.

From Table 2, one notices that, for the present example, 4 rules are set

*Rule* 1: IF $E$ is PS and $\dot{E}$ is Z, THEN $V$ is NS;

*Rule* 2: IF $E$ is PS and $\dot{E}$ is P, THEN $V$ is NS;

*Rule* 3: IF $E$ is PM and $\dot{E}$ is Z, THEN $V$ is NM;

*Rule* 4: IF $E$ is PM and $\dot{E}$ is P, THEN $V$ is NM.

The effects of the AND operation (or "Mamdani's minimum operation") associated with each rule on the output fuzzy sets are shown in Figures 5, 6, 7 and 8. Each hatched trapezoid represents the configuration of the output fuzzy set, for a given rule. The global configuration of the output fuzzy set, for all 4 rules, is shown in Figure 9, where the OR operation is applied. The hatched zone represents the figure created by putting together

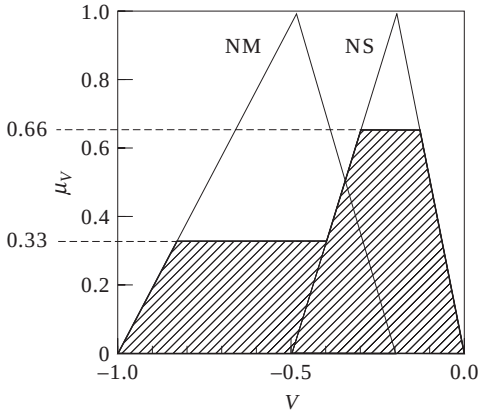


Figure 9. The output fuzzy set after the AND operation.

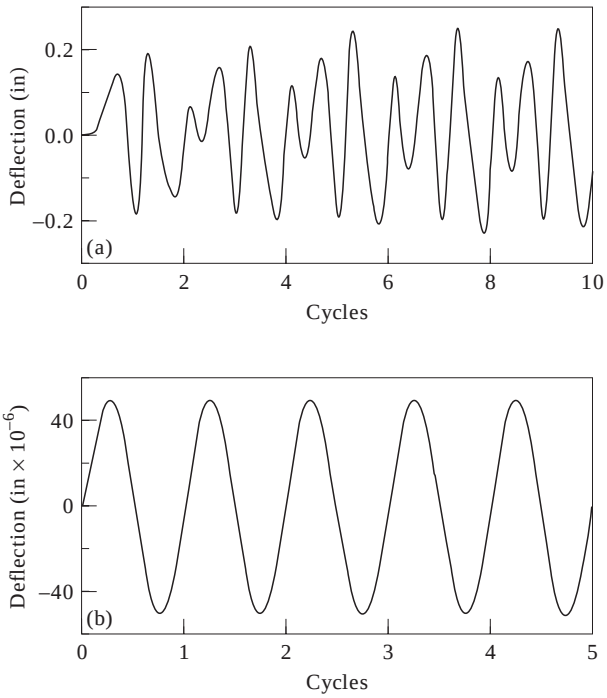


Figure 10. (a) Uncontrolled and (b) controlled mid span deflection for 1435 r.p.m.

all the four trapezoid from Figures 5, 6, 7 and 8. It should be noticed that overlapped areas are eliminated.

### 3.3. DEFUZZIFICATION

The fuzzy output is converted to a crisp or exact numerical value of output for input to control the process or plant (after scaling).

The output of the fuzzy controller is a fuzzy variable defined here on the interval $[-1, 1]$ and convertible into the non-fuzzy variable $V$ by a process called *defuzzification* (performed in the block DFI in Figure 3). The defuzzification block is aimed at creating a numerical-valued non-fuzzy control action that best represents a fuzzy control action. In this paper, the common method called "center of area method" is applied.

For the considered example, the normalized control voltage $V$ of the specific actuator is the horizontal co-ordinate of the center of gravity of the hatched zone from Figure 9. The actual voltage $U$ is computed using equation (29).

## 4. SIMULATIONS AND RESULTS

Parameters of that apparatus were chosen to be from reference [1]: aluminum rod length $L = 11{\cdot}5$ in; rod cross-section $0{\cdot}75$ in $\times$ $0{\cdot}0603$ in; and a damping ratio $= 0{\cdot}02$ for the first and $0{\cdot}04$ for the second and third modes, respectively; piston mass $M_s = 0{\cdot}478$ lbm, and rod mass per unit length $= 0{\cdot}0045$ lbm/in. Membership functions and fuzzy sets used were those in Figures 4 and 5. In this study, the scaling factors were chosen after trial-and-error to be $GE = 10^4$ when $|y_k| < 10^{-4}$, otherwise, $GE = 10$; $GC = 1$ and $GU = 1500$.

Figures 10(a) and 10(b) show the uncontrolled and controlled midspan deflection of the connecting-rod for a $0{\cdot}25$ in crank running at 1435 r.p.m. The horizontal axis represents

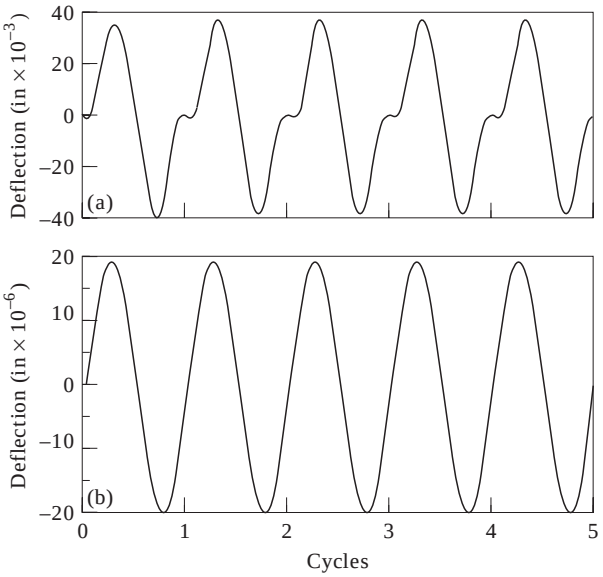


Figure 11. (a) Uncontrolled and (b) controlled mid span deflection for 912 r.p.m.

the time in cycles, where one cycle corresponds to one rotation of the crank. Experimentally the authors have observed that under these conditions the response period doubled and hence the system is unstable, as shown in Figure 10(a) from Halbig and Beale [1]. When the fuzzy logic controller is applied, the amplitude of the deflection decreases to 50 μin.

Figures 11(a) and 11(b) show the uncontrolled and controlled mid-span response of the connecting-rod when the crank length is 0·25 in and running at 912 r.p.m. The

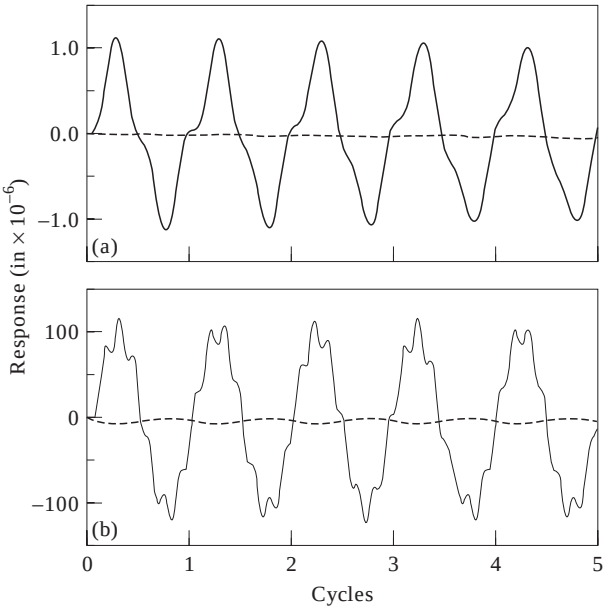


Figure 12. (a) Second mode and (b) third mode response for 912 r.p.m.: ——, without control input; – – –, with control input.

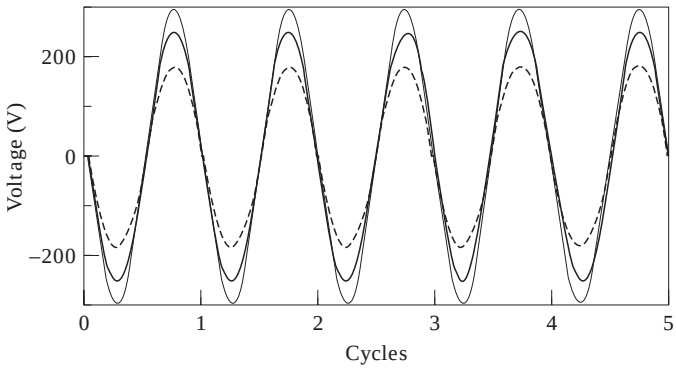


Figure 13. Applied voltages on actuators: ——, first actuator; ——, second actuator; – – –, third actuator.

uncontrolled response amplitude was about 0·04 in midspan deflection. In both instances, the rod is initially started without transverse deflection and velocity of deflection. It reveals that the midspan deflection is reduced quickly by this control scheme. Figures 12(a) and 12(b) show the time variation of the second and third mode, respectively. Although the second and third modes are not important contributors to the total response of the uncontrolled beam, the possibility exists that a controller may excite these higher modes. However, Figures 12(a) and 12(b) show that the second and third mode response is indeed controlled, and are strongly suppressed by this controller. Figure 13 shows the corresponding input voltage applied to the three piezo-actuators. Note that peak voltages are below the breakdown voltage of the piezo-material at $\pm 1500$ volts.

The robustness of the control scheme is tested by including unmodellable disturbance effects as a randomized sine function in equation (15) which has the form $\mathbf{d} = [\mathbf{d}_q \ \mathbf{d}_\phi \ \mathbf{d}_s]^{\mathrm{T}}$. The randomized sine function is

$$d = D \times rand \times \sin \omega t, \tag{30}$$

where *rand* is the random number and $D$ is the amplitude. The response of the controlled system to no disturbance and disturbance with $D$ equalling 10% are plotted in Figure 14 for the speed again equalling 912 r.p.m., for the crank size 0·25 in. This plot shows that the proposed control law is able to contain undesired disturbances while still keeping the response small.

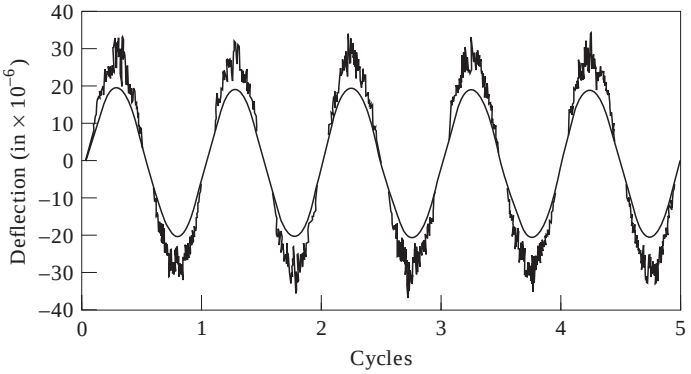


Figure 14. Mid span deflection for random noise for 912 r.p.m.: ——, without noise; ——, with noise ($D = 10\%$).

## 5. CONCLUSIONS

Research has not been focussed on flexible mechanism control in the presence of non-linearities. Even though the traditional linear control laws have been applied to flexible mechanisms, they may not be suitable when the non-linearities are not negligible. In this paper, the application of fuzzy control for flexible mechanisms is explored. Fuzzy logic is found to be quite suitable. From the numerical simulation, the transverse deflection of the flexible link was significantly reduced by a fuzzy control algorithm. The next logical step is experimental work.

## REFERENCES


1. D. Halbig and D. G. Beale 1995 *Nonlinear Dynamics* **7**, 364–384. Experimental observations of a flexible slider crank mechanism at high speeds.
2. W. L. Cleghorn, R. G. Fenton and B. Tabarrok 1981 *Mechanism and Machine Theory* **16**, 389–406. Optimum design of high speed flexible mechanisms.
3. A. J. Kakatsio and S. J. Tricamo 1987 *American Society of Mechanical Engineers*, *Journal of Mechanisms*, *Transmissions*, *and Automation in Design* **109**, 338–347. Integrated kinematic and dynamic optimal design of flexible planar mechanisms.
4. C. K. Sung and B. S. Thompson 1984 *Mechanism and Machine Theory* **19**, 389–396. Material selection—an important parameter in the design of high speed linkages.
5. J. H. Oliver, D. A. Wysocki and B. S. Thompson 1985 *Mechanism and Machine Theory* **20**, 103–114. The synthesis of flexible linkages by balancing the tracer point quasistatic deflections using microprocessors and advanced materials technologies.
6. C. A. Rogers, O. K. Barker and C. A. Jager 1988 *Smart Materials*, *Structures*, *and Mathematical Issues*. Introduction to smart materials and structures (editor Craig A. Rogers). Westport, CT: Technomic Publishing Co.
7. T. Bailey and J. E. Hubbard, Jr. 1985 *Journal of Guidance*, *Control and Dynamics* **8**, 605. Distributed piezoelectric polymer active vibration control of a cantilever beam.
8. H. S. Tzou and M. Gadre 1989 *Journal of Sound and Vibration* **132**, 433–450. Theoretical analysis of multi-layered thin shell actuators for distributed vibration controls.
9. C. K. Sung and Y. C. Chen 1991 *Journal of Vibration and Acoustics* **113**, 14–21. Vibration control of the elastodynamic response of a high speed flexible linkage mechanism.
10. C. Y. Lee, S. R. Choi, B. S. Thompson and M. V. Gandhi 1989 *Proceedings of the First National Applied Mechanisms and Robotics Conference*, 89AMR-2C-1, Cincinnati, Ohio. A variational formulation for the finite element analysis and control of linkage and robotic systems featuring smart material incorporating piezoelectric materials.
11. C. Y. Liao and C. K. Sung 1993 *Transactions of the American Society of Mechanical Engineers*, *Journal of Mechanical Design* **115**, 658–665. An elastodynamic analysis and control of flexible linkages using piezoceramic sensors and actuators.
12. B. S. Thompson and X. Tao 1995 *Journal of Sound and Vibration* **187**, 718–723. A note on the experimentally determined elastodynamic response of a slider-crank mechanism featuring a macroscopically smart connecting rod with ceramic piezoelectric actuators and strain gauge sensor.
13. K. Liu and F. Lewis 1992 *Proceedings of SINS' International Symposium Implicit Nonlinear Systems*, 21–26. Fuzzy logic control of a flexible link manipulator.
14. E. Kubica and D. Wang 1993 *American Control Conference Proceedings*, 236–241. A fuzzy control strategy for a flexible single link robot.
15. D. Beale and S. W. Lee 1996 *Mechanism and Machine Theory* **31**, 215–227. Nonlinear equation instability boundaries in flexible mechanisms.
16. C. M. Lim and T. Hiyama 1991 *Institute of Electrical and Electronic Engineers*, *Transactions on Robotics and Automation* **7**, 688–691. Application of fuzzy logic control to a manipulator.
17. D. Boghiu and D. Marghitu 1996 accepted for publication in the *Journal of Vibration and Control*. Control of an impacting rotating flexible beam.
18. D. Boghiu, D. Marghitu and S. C. Sinha 1996 *The Sixth Conference on Nonlinear Vibrations*, *Stability and Dynamics of Structures*, *Blacksburg*, *Virginia*. Stability and control of a parametrically excited rotating beam.

19. J. L. Fanson and T. K. Caughey 1990 *American Institute of Aeronautics and Astronautics Journal* **28**, 717–724. Positive position feedback control for large space structures.
20. E. Garcia and D. J. Inman 1990 *Journal of Intelligent Materials Systems and Structures* **1**, 261–272. Advantages of slewing and active structure.
21. C. F. Lin 1994 *Advanced Control Systems Design*. Englewood Cliffs, New Jersey: Prentice Hall.